Anti-metastatic effect of ^{131}I-labeled *Buthus martensii* Karsch chlorotoxin in gliomas

SHAN WU[1*], KE MA[2*], WEN-LI QIAO[1*], LING-ZHOU ZHAO[1], CHANG-CUN LIU[1], LI-LEI GUO[1], YAN XING[1], MEI-LIN ZHU[3] and JIN-HUA ZHAO[1]

[1]Department of Nuclear Medicine, Shanghai General Hospital, Shanghai Jiao Tong University School of Medicine, Shanghai 200080; [2]Shandong Co-Innovation Center of Classic TCM Formula, Shandong University of Traditional Chinese Medicine, Jinan, Shandong 250355; [3]School of Basic Medical Sciences, Ningxia Medical University, Yinchuan, Ningxia 750004, P.R. China

Received June 11, 2018; Accepted September 27, 2018

DOI: 10.3892/ijmm.2018.3905

Abstract. The present study investigated the underlying molecular mechanism by which *Buthus martensii* Karsch chlorotoxin (BmK CT) inhibits the invasion and metastasis of glioma cells and the possibility of ^{131}I-labeled BmK CT (^{131}I-BmK CT) as a novel targeted agent for the treatment of glioma. The impact of BmK CT with and without ^{131}I radiolabeling on the invasion and metastasis of glioma cells *in vitro* was studied. Cell viability was assessed using Cell Counting Kit-8 and plate colony formation assays in order to confirm the cytotoxicity of BmK CT and ^{131}I-BmK CT at different concentrations. Transwell invasion and wound-healing assays were conducted in order to investigate the inhibitory effects BmK CT and ^{131}I-BmK CT on cell migration and invasion. Furthermore, western blotting, ELISA immunofluorescence and a gelatin zymography assay were performed to evaluate changes in the protein expression levels of glioma cells following treatment with BmK CT or ^{131}I-BmK CT. The results indicated that BmK CT inhibits the invasion and metastasis of glioma cells via regulation of tissue inhibitor of metalloproteinase-2 expression and that ^{131}I-BmK CT has the potential to be a novel targeted therapeutic drug for glioma.

Correspondence to: Professor Jin-Hua Zhao, Department of Nuclear Medicine, Shanghai General Hospital, Shanghai Jiaotong University School of Medicine, 100 Haining Road, Shanghai 200080, P.R. China
E-mail: zhaojinhua1963@126.com

Professor Mei-Lin Zhu, School of Basic Medical Sciences, Ningxia Medical University, 1160 Shengli Street, Yinchuan, Ningxia 750004, P.R. China
E-mail: jay70281@163.com

*Contributed equally

Key words: Buthus martensii Karsch chlorotoxin, ^{131}I, glioma, metastasis, mechanism

Introduction

Glioma accounts for 80% of malignant brain tumors and has one of the highest mortality rates among all types of cancer (1). The current standard glioma treatment comprises surgical excision followed by radiotherapy and chemotherapy (2). However, as glioma cells infiltrate into the brain parenchyma, combination therapy can only minimally prolong survival time and almost all patients relapse (3-5). The high risk of recurrence following combination therapy is a major therapeutic challenge. Thus, it is necessary to investigate novel therapeutic approaches to glioma and the underlying mechanism of the invasion and metastasis of glioma cells.

Tumor metastasis is a multi-step process that comprises neovascularization and cell adhesion, invasion, migration and proliferation, in which the crucial step is degradation of the extracellular matrix (ECM) and basement membrane (6,7). A growing body of evidence supports the perspective that tumor progression is associated with the overexpression of matrix metalloproteinases (MMPs) in tumor cells, particularly that of MMP-2 and -9, which are able to modulate the tumor microenvironment (8). Apart from their role in the degradation of the ECM and cancer metastasis, MMPs also regulate inflammatory processes, cell proliferation and angiogenesis (9). These functions of MMPs provide an alternative method for targeting cancer therapy. There are multiple methods to regulate the activities of MMPs, including regulation of the following: MMP mRNA expression, conversion from the zymogen to the active enzyme, and tissue inhibitors of metalloproteinases (TIMPs) (9). A number of studies have demonstrated that overexpression of TIMPs can reduce tumor metastasis (10-12). In the TIMP family, TIMP-1 and -2 are able to suppress the activities of most known MMPs (11).

Peptide toxins have offered a novel approach for targeted treatment of glioma. Chlorotoxin (CTX), a 36-amino-acid peptide that is isolated from the venom of *Leiurus quinquestriatus* (13), has been considered to be a novel blocker of small conductance chloride ion channels (14) and MMP-2 (15). It has an anti-invasive effect that is due to inhibition of the enzymatic activity of MMP-2 and reduced expression of MMP-2 via its interactions with MMP-2 (15).

Furthermore, ^{131}I-labeled CTX is considered to be a promising agent for imaging or therapy of glioma (16-18) and has been used in clinical trials (19,20). Similarly, a CTX-like peptide purified from *Buthus martensii* Karsch (BmK CT), which possesses similar biological features to CTX, has been demonstrated to inhibit glioma cell proliferation, migration and invasion (21). Our previous studies have revealed that BmK CT can specifically bind to C6 glioma cells and suppress cell invasion through downregulation of MMP-2 expression (22-24), while not affecting mRNA expression of MMP-2 at the genetic level (24). However, these studies only investigated the MMP-2 protein. Thus, the aim of the present study was to further investigate the potential anti-metastasis mechanism of BmK CT on glioma cells and the possibility of ^{131}I-labeled BmK CT (^{131}I-BmK CT) as a novel targeted therapeutic agent for glioma.

In the present study study, Cell Counting Kit-8 (CCK-8) and plate colony formation assays demonstrated that BmK CT had no influence on cell proliferation at concentrations of 0-1 mg/ml, while a significant reduction in proliferation was observed in the glioma cells treated with ^{131}I-BmK CT. Furthermore, the results of the cell cycle assay demonstrated that only ^{131}I-BmK CT could induce evident changes in the cell cycle and arrest glioma cells at the S and G_2/M phases. Transwell invasion and wound healing assays demonstrated that ^{131}I-BmK CT possessed a stronger effect than BmK CT in terms of inhibiting cell migration and invasion. Furthermore, western blotting, ELISA, immunofluorescence and a gelatin zymography assay demonstrated that both ^{131}I-BmK CT and BmK CT were able to downregulate the expression of MMP-2 and -9 proteins, and upregulate that of TIMP-2 protein. Notably, ^{131}I-BmK CT was more effective than BmK CT at inhibiting cell migration and invasion and the enzyme activity of MMP-2 and -9, but not at inhibiting the protein expression of MMP-2, MMP-9 and TIMP-2. The results indicate that BmK CT inhibits the metastasis of U87MG cells via regulation of TIMP-2 expression and that ^{131}I-BmK CT has the potential to be a novel targeted drug for glioma therapy.

Materials and methods

Materials. U87MG cells (CVCL_0022), human glioblastoma cells of unknown origin, were purchased from American Type Culture Collection (Manassas, VA, USA). Dulbecco's modified Eagle's medium (DMEM), fetal bovine serum (FBS), streptomycin, penicillin and CCK-8 were purchased from Shanghai DoBio Biotech Co., Ltd. (Shanghai, China). Rabbit anti-MMP-2 (cat. no. 40994), -MMP-9 (cat. no. 13667) and -TIMP-2 (cat. no. 5738) monoclonal antibodies were purchased from Cell Signaling Technology, Inc. (Danvers, MA, USA). PI/RNase staining buffer and mouse anti-β-actin antibody were obtained from Beyotime Institute of Biotechnology (Haimen, China). BmK CT was purchased from Chinese Peptide Company, Ltd. (Hangzhou, China). Na^{131}I solution was supplied by Shanghai GMS Pharmaceutical Co., Ltd. (Shanghai, China). Disposable PD-10 desalting columns were procured from GE Healthcare (Chicago, IL, USA). All other chemicals and solvents were supplied by Sinopharm Chemical Reagent Co., Ltd. (Shanghai, China).

Synthesis of ^{131}I-BmK CT. For the ^{131}I radiolabeling, a tyrosine was modified in the N-terminus of BmK CT that could be labeled with ^{131}I easily using the chloramine-T method. Briefly, sterile Na^{131}I solution (370-740 MBq; 0.1-0.2 ml) was mixed with 0.2 ml PBS containing BmK CT (200 μg) and chloramine-T (100 μg). The mixture was continuously stirred for 5 min at room temperature and then 100 μg $Na_2S_2O_5$ was added to stop the reaction. Subsequently, ^{131}I-BmK CT was purified from the reaction mixture using disposable PD-10 desalting columns. In the follow-up experiments, the specific activity was 10 mCi/mg.

Cell proliferation assay. U87MG cells were cultured in DMEM supplemented with 10% FBS, 1% streptomycin and 1% penicillin at 37˚C with 5% CO_2 as described previously (25,26). Cell viability was examined using a CCK-8. Briefly, U87MG cells were seeded in 96-well plates (5,000 cells/well) and treated with different concentrations of BmK CT (0, 0.1, 1, 10, 100 and 1,000 μg/ml) or ^{131}I-BmK CT (0, 12.5, 25, 50, 100 and 200 μCi/ml) for 24, 48 and 72 h at 37˚C. CCK-8 solution (10 μl) was then added to each well and cells were incubated for a further 1 h at 37˚C. Subsequently, the absorbance at 450 nm was measured using a Gen5 microplate reader (BioTek Instruments, Inc., Winooski, VT, USA).

Plate colony formation assay. In order to evaluate colony formation, 400 log-phase U87MG cells were seeded in 6-well plates and then treated with BmK CT (0, 0.05, 0.5, 5, 10 and 20 μg/ml) or ^{131}I-BmK CT (0, 0.5, 5, 50, 100 and 200 μCi/ml) for 24 h. Subsequently, the culture medium was replaced with fresh culture medium. Following incubation at 37˚C for 10 days, the cells were fixed in methyl alcohol and stained with crystal violet for 15 min at room temperature. The colonies were then counted and images of the plates were captured.

Cell cycle analysis. U87MG cells were seeded at a density of $2x10^5$ cells/ml in 6-well culture plates and then were treated with different concentrations of BmK CT (0, 5, 10 and 20 μg/ml) or ^{131}I-BmK CT (0, 50, 100 and 200 μCi/ml). Following incubation for 72 h at 37˚C, the cells were trypsinized, washed twice with PBS and fixed with 70% ethanol overnight at 4˚C. The cells were then resuspended in PI/RNase staining buffer for 30 min at 37˚C and analyzed using flow cytometry (BD Accuri C6 Software; version 1. 0. 264. 21; BD Biosciences, San Jose, CA, USA).

Transwell invasion assay. Transwell inserts (Corning Incorporated, Corning, NY, USA) were coated with Matrigel (BD Biosciences) to form a thin layer of gel and incubated overnight at 37˚C. U87MG cells were treated with PBS, Na^{131}I (0.5, 5 and 50 μCi/ml), BmK CT (0.05, 0.5 and 5 μg/ml) or ^{131}I-BmK CT (0.5, 5 and 50 μCi/ml) for 24 h. A total of $5x10^4$ cells were seeded in the upper chamber with serum-free DMEM medium and then the chambers were placed into a 24-well plate containing complete medium. Following incubation for 24 h at 37˚C, cells on the upper surface of the chambers were removed with a cotton swab and the chambers were washed 3 times with PBS. Subsequently, the cells on the lower surface of the chambers were fixed with methanol for 15 min and stained with crystal violet solution for 30 min at 37˚C.

The number of invaded cells was counted under an inverted microscope (magnification, x200).

Wound healing assay. U87MG cells were seeded at a density of $4x10^5$ cells/ml in a 6-well plate to form a confluent monolayer. A wound was made with a pipette tip and then fresh medium containing the treatment (PBS, 50 μCi/ml $Na^{131}I$, 5 μg/ml BmK CT or 50 μCi/ml ^{131}I-BmK CT) was added to the wells. Then the cells were incubated at 37˚C. Images of the cells were captured at 0, 12 and 24 h with an inverted phase contrast microscope, and cell migration was assessed by measuring the size of the gap in multiple fields. The microscope images were quantified by a distance measurement. The magnification of the microscope was set as x100.

Western blotting assays. The primary antibodies used were rabbit anti-MMP-2, -MMP-9 and -TIMP-2 (1:1,000). Horseradish peroxidase-conjugated goat anti-mouse or anti-rabbit secondary antibodies (cat. no. 7076 and 7074; 1:10,000; Cell Signaling Technology, Inc.) were used to detect the primary antibodies on the western blots. Briefly, cells were incubated with PBS, BmK CT (5 μg/ml), $Na^{131}I$ or ^{131}I-BmK CT (50 μCi/ml) for 72 h at 37˚C. Total protein from the U87MG cells was isolated using radioimmunoprecipitation assay lysis buffer (Beyotime Institute of Biotechnology) and the protein concentration was measured using a bicinchoninic acid protein assay kit (Beyotime Institute of Biotechnology). A total of 20 μg total protein was separated by 10% SDS-PAGE and transferred onto a polyvinylidene difluoride (PVDF) membrane. The PVDF membranes weres then blocked in PBS containing 5% skimmed milk and 0.1% Tween-20 for 2 h at room temperature. Subsequently, the membranes were incubated at 4˚C overnight with the primary antibodies, followed by incubation with the corresponding secondary antibody for 1 h at room temperature. The bands were visualized with enhanced chemiluminescence reagents (Beyotime Institute of Biotechnology). The expression of the proteins was quantified using ImageJ software (version 1.52a; National Institutes of Health, Bethesda, MD, USA) and compared with that of the control (β-actin).

Confocal microscopy. U87MG cells were seeded at a density of $5x10^4$ cells/ml in glass bottom cell culture dishes. The cells were initially incubated in medium containing the treatment for 48 h and the incubation conditions were the same as those of the western blotting assay. Subsequently, cells were fixed with 4% paraformaldehyde solution for 15 min at room temperature. The cells were then washed 3 times with PBS, permeabilized with 0.2% Triton X-100 for 15 min at 37˚C and blocked with 5% bovine serum albumin (cat. no. P0260; Shanghai DoBio Biotech Co., Ltd.) in PBS for 30 min at room temperature. Following blocking, cells were incubated with the appropriate primary antibody (MMP-2, MMP-9 and TIMP-2; 1:250) overnight at 4˚C. The cells were then washed 3 times with PBS and stained with fluorescein isothiocyanate-labelled goat anti-rabbit immunoglobulin G (cat. no. SAB3700873; 1:300; Sigma-Aldrich; Merck KGaA, Darmstadt, Germany) for 1 h at 37˚C. Subsequently, the cells were washed 3 times with PBS and were then stained with DAPI for 2 min at room temperature. Images were captured using a confocal microscope (FV300; Olympus Corporation, Tokyo, Japan).

ELISA. Rat MMP-2, MMP-9 and TIMP-2 ELISA kits were purchased from Sigma-Aldrich (cat. nos. RAB1916, RAB1112 and RAB1156, respectively; Merck KGaA). U87MG cells were treated with BmK CT (0.05, 0.5 and 5 μg/ml), $Na^{131}I$ or ^{131}I-BmK CT (0.5, 5 and 50 μCi/ml) for 72 h at 37˚C. The secreted proteins MMP-2, MMP-9 and TIMP-2, which are produced by U87MG cells, in the supernatant from each well were evaluated via ELISA. Briefly, 96-well ELISA plates were coated with the appropriate antibodies (MMP-2, MMP-9 and TIMP-2) at 4˚C overnight. Subsequently, the supernatants of the cell cultures (100 μl) collected by centrifugation (3,661 x g; 15 min; 4˚C) were added to the plates and the plates were incubated for 1 h at 37˚C. The plates were washed 5 times with PBS and then incubated with the horseradish peroxidase-conjugated detection antibodies provided with each kit for 1 h at 37˚C. The plates were washed a further 5 times and were then incubated for 15 min at 37˚C with tetramethyl benzidine dilution. The reaction was stopped with 2N H_2SO_4 and the absorbance at 450 nm was determined using a microplate reader (BioTek Instruments, Inc.).

Gelatin zymography assay. The activities of MMP-2 and -9 were examined using a gelatin zymography assay. U87MG cells were treated with PBS, BmK CT (0.05, 0.5 and 5 μg/ml) or ^{131}I-BmK CT (0.5, 5 and 50 μCi/ml) for 72 h at 37˚C. Protein was isolated and the concentration determined as in the western blotting protocol. Total protein (10 μg) was separated using 10% SDS-PAGE that included 1% gelatin (Invitrogen; Thermo Fisher Scientific, Inc., Waltham, MA, USA) without prior heating or reduction. The gel was washed with 2.5% Triton-X 100 to strip the SDS and incubated with developing buffer (50 mM Tris-HCl, 150 mM NaCl and 5 mM $CaCl_2$) for 16 h at 37˚C. Following staining with 0.5% Coomassie Brilliant Blue R-250 (Sigma-Aldrich; Merck KGaA) for 3 h at room temperature, the gel was destained and photographed. Signal intensities were measured by densitometry using Bio-1D software, version 15.01 (Vilber Lourmat Deutschland GmbH, Eberhardzell, Germany).

Statistical analysis. Data are presented as the mean ± standard deviation. All results were analyzed using SPSS software, version 20.0 (IBM Corp., Armonk, NY, USA). Student's t-test was used to analyze the variances between two groups. Multi-group comparisons of the means were carried out by one-way analysis of variance. $P<0.05$ was considered to indicate a statistically significant difference.

Results

^{131}I-BmK CT inhibits U87MG cell proliferation. In order to investigate the proliferation of U87MG cells treated with BmK CT or ^{131}I-BmK CT, CCK-8 and plate colony formation assays were performed. The viability of the U87MG cells did not change significantly following treatment with BmK CT at concentrations of 0-1,000 μg/ml (Fig. 1Aa-c). However, there was significant inhibition in the growth of the cells in the ^{131}I-BmK CT group. This effect was time- (24-72 h) and

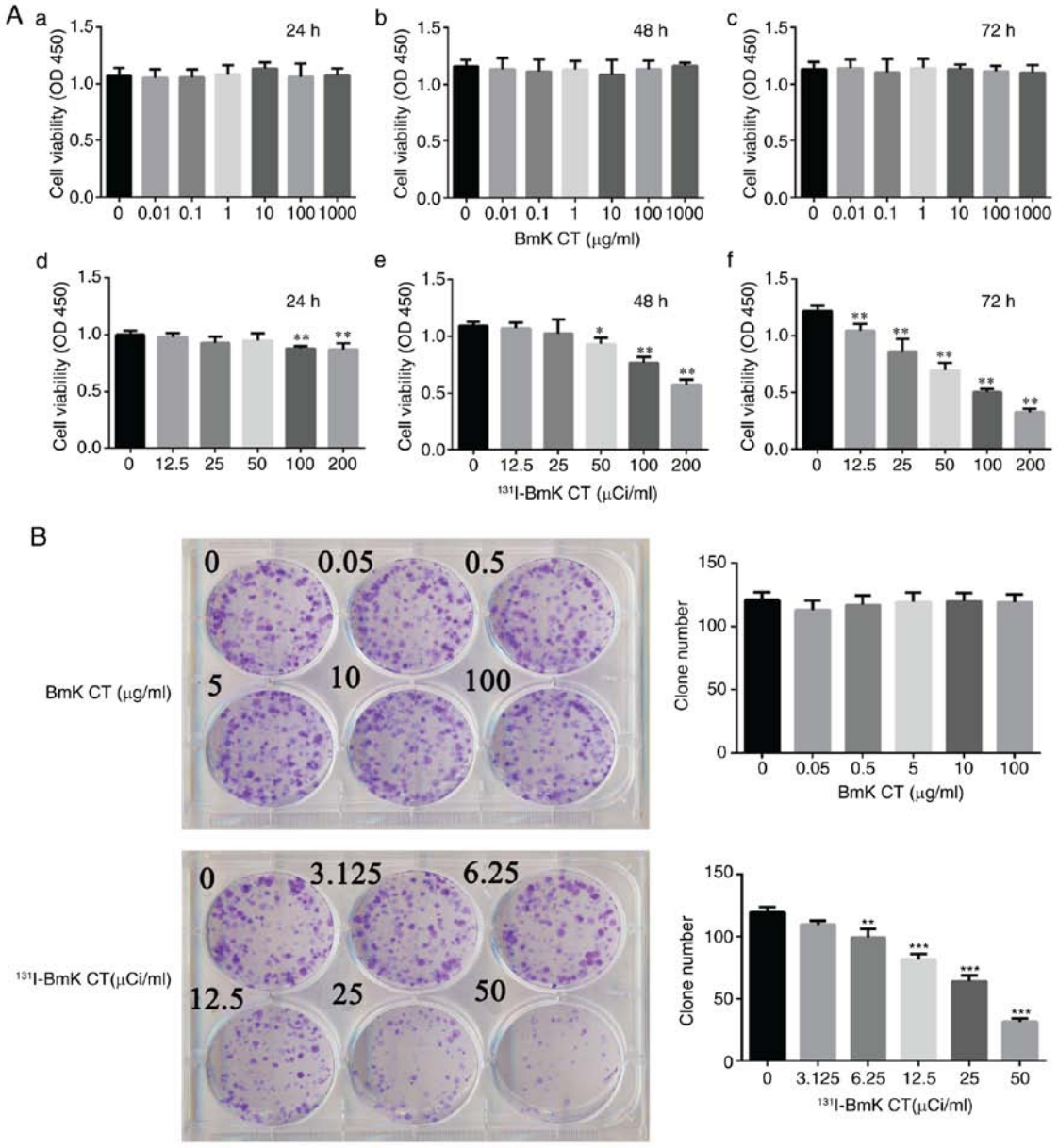

Figure 1. Effect of BmK CT and ^{131}I-BmK CT on U87MG cells. (A) Cell growth was inhibited by ^{131}I-BmK CT in a dose- and time-dependent manner. Incubated with BmK CT for (a) 24 h, (b) 48 h and (c) 72 h; incubated with ^{131}I-BmK CT for (d) 24 h, (e) 48 h and (f) 72 h. (B) U87MG cells treated with ^{131}I-BmK CT exhibited weaker clone formation. *P<0.05, **P<0.01 and ***P<0.001 vs. 0 μCi/ml. BmK CT, *Buthus martensii* Karsch chlorotoxin; ^{131}I-BmK CT, ^{131}I-labeled BmK CT; OD, optical density.

dose-dependent (0-200 μCi/ml; Fig. 1Ad-f). The half maximal inhibitory concentration of the ^{131}I-BmK CT cells at the 72-h time point was 50 μCi/ml. In addition, the colony formation assay demonstrated that ^{131}I-BmK CT reduced colony formation compared with the blank control (Fig. 1B). These results demonstrated that ^{131}I-BmK CT could inhibit U87MG cell proliferation, whereas BmK CT had no significant influence on cell viability at a concentration of ≤1,000 μg/ml.

^{131}I-BmK CT induces changes in the cell cycle of U87MG cells. As presented in Fig. 2A, BmK CT (0, 5, 10 and 20 μg/ml) did not significantly affect the cell cycle progression of U87MG cells. In contrast to blank control, ^{131}I-BmK CT (50, 100 and 200 μCi/ml) significantly increased the proportion of U87MG cells in the S and G_2/M phases and reduced the proportion of cells in the G_1 phase (Fig. 2B). These results suggest that ^{131}I-BmK CT inhibits cell proliferation by inducing cell cycle arrest at the S and G_2/M phases.

^{131}I-BmK CT inhibits U87MG cell invasion and migration. Tumor metastasis depends on the capacity of tumor cells to invade and migrate to distant sites. Transwell invasion assays demonstrate the invasive capacity of tumor cells. The results in the present study demonstrated that the number of cells that passed through the membrane was reduced following treatment with BmK CT and ^{131}I-BmK CT. As the treatment concentration increased, a significant reduction in the cell number was observed (Fig. 3A). As presented in Fig. 3B, the results of wound healing assay *in vitro* demonstrated that 24 h following scraping, the cells in the PBS group had migrated across the wound. The percentage of wound closure in the Na^{131}I, BmK CT and ^{131}I-BmK CT groups was 78.3±19.6,

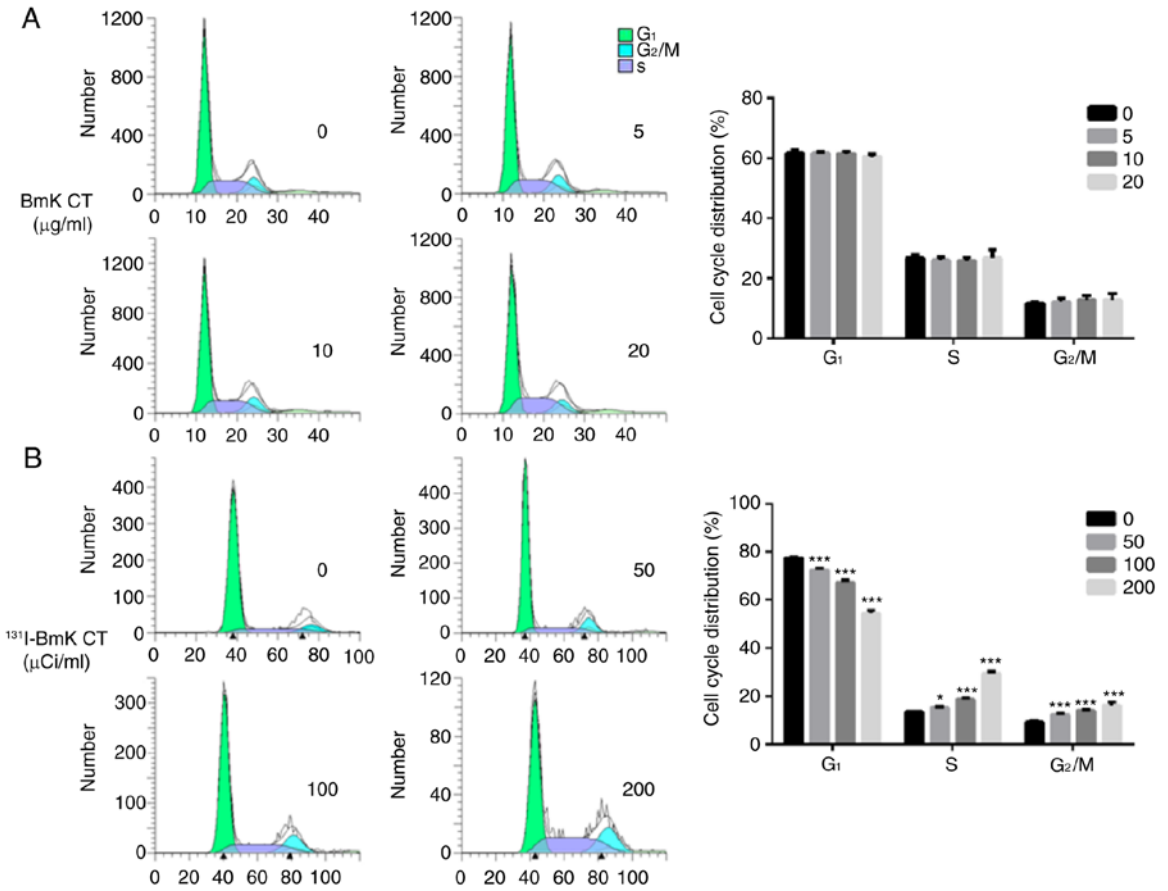

Figure 2. Effect of BmK CT and ^{131}I-BmK CT on the cell cycle. (A) BmK CT did not significantly affect the cell cycle progression of U87MG cells. (B) ^{131}I-BmK CT induced arrest at the S and G_2/M phases and reduced the number of cells in the G_1 phase compared with the control group. *P<0.05 and ***P<0.001 vs. 0 μCi/ml. BmK CT, *Buthus martensii* Karsch chlorotoxin; ^{131}I-BmK CT, ^{131}I-labeled BmK CT.

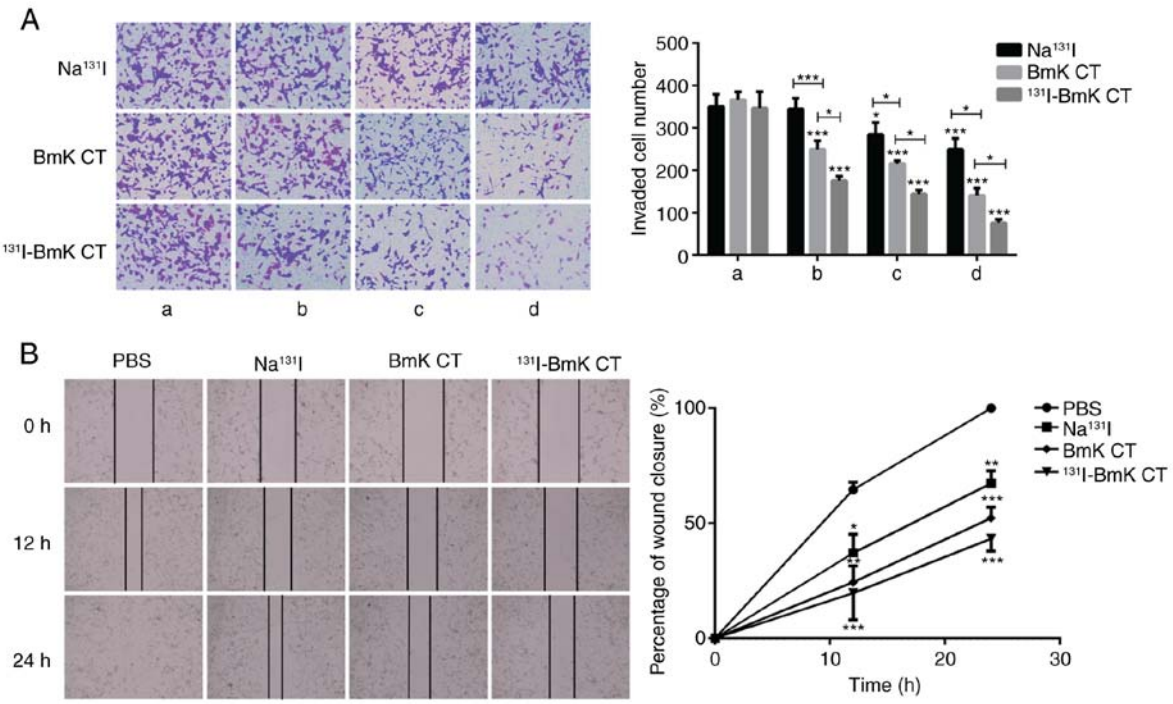

Figure 3. BmK CT inhibited U87MG cell invasion and migration. (A) The number of invaded cells was significantly lower in the groups treated with BmK CT or ^{131}I-BmK CT. The concentration of group BmK CT was (a) 0, (b) 0.05, (c) 0.5 and (d) 5 μg/ml. The concentration of group ^{131}I-BmK CT was (a) 0, (b) 0.5, (c) 5 and (d) 50 μCi/ml (The specific activity was 10 mCi/ml). The concentration of group Na^{131}I was (a) 0, (b) 0.5, (c) 5 and (d) 50 μCi/ml. Magnification, x200. (B) Migration of U87MG cells following the different treatments was detected using a wound-healing assay (magnification, x100). *P<0.05, **P<0.01 and ***P<0.001. BmK CT, *Buthus martensii* Karsch chlorotoxin; ^{131}I-BmK CT, ^{131}I-labeled BmK CT.

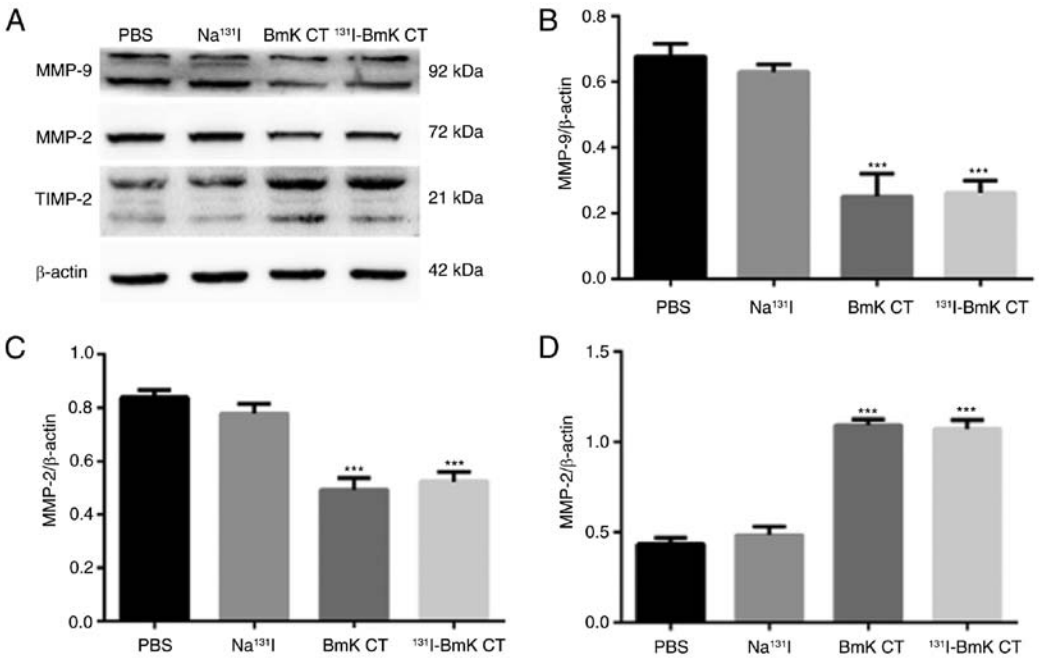

Figure 4. The expression of MMP-9, MMP-2 and TIMP-2 in U87MG cells was determined using (A) western blotting, and (B-D) densitometry values were evaluated. ***P<0.001 vs. PBS. MMP, matrix metalloproteinase; TIMP, tissue inhibitor of metalloproteinases; BmK CT, *Buthus martensii* Karsch chlorotoxin; ^{131}I-BmK CT, ^{131}I-labeled BmK CT.

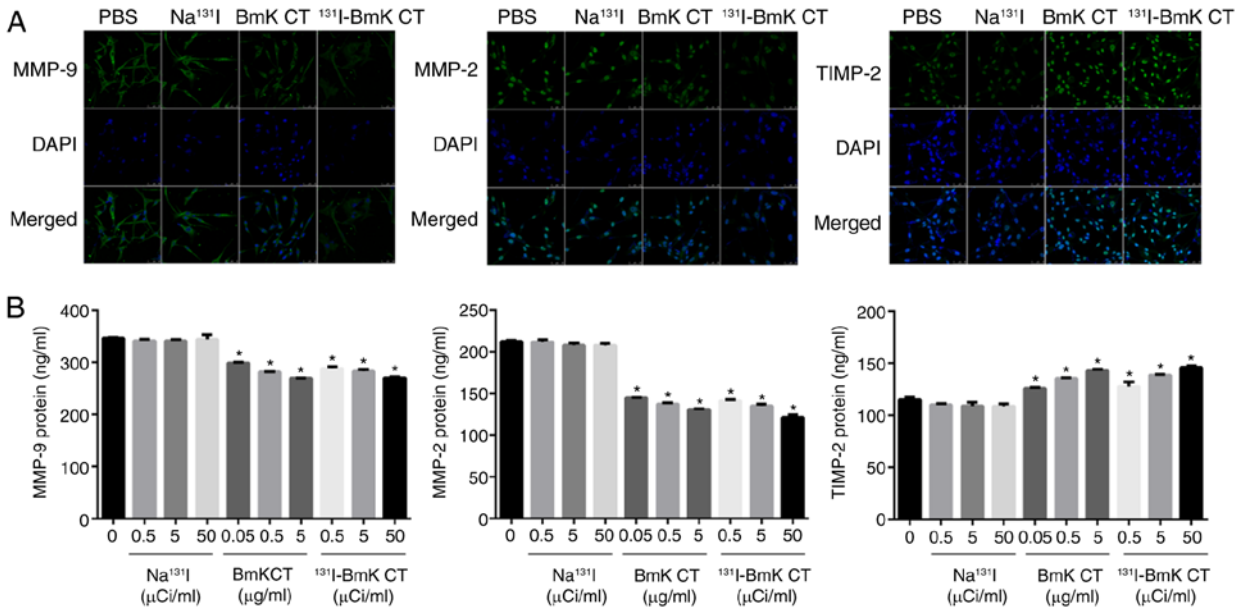

Figure 5. BmK CT regulates the expression of MMP-9, MMP-2 and TIMP-2 in U87MG cells. (A) The expression levels were analyzed using immunofluorescence (magnification, x400). (B) The protein concentrations secreted by the U87MG cells were evaluated using ELISA. *P<0.05 vs. 0. *Buthus martensii* Karsch chlorotoxin; MMP, matrix metalloproteinase; TIMP, tissue inhibitor of metalloproteinases; ^{131}I-BmK CT, ^{131}I-labeled BmK CT.

56.6±10.0 and 45.0±8.2%, respectively, and these results were statistically significant compared with the blank control. The Transwell and wound healing assays demonstrated that BmK CT can inhibit the invasion and migration of U87MG cells, and that ^{131}I-BmK CT has a more marked effect than BmK CT at the same concentration.

^{131}I-BmK CT regulates the expression of MMP-2, MMP-9 and TIMP-2 in U87MG cells. Western blotting demonstrated that BmK CT upregulated TIMP-2 and downregulated MMP-2 and -9 in U87MG cells compared with the blank control (Fig. 4). These results indicate that BmK CT upregulates TIMP-2 and downregulates MMP-2 and -9. Furthermore, ^{131}I-BmK CT was not significantly more effective than BmK CT. The upregulation of TIMP-2 and downregulation of MMP-2 and -9 were also visualized by confocal imaging of the U87MG cells (Fig. 5A).

^{131}I-BmK CT stimulates the secretion of TIMP-2 and suppresses the expression of MMP-2 and -9. ELISA was used

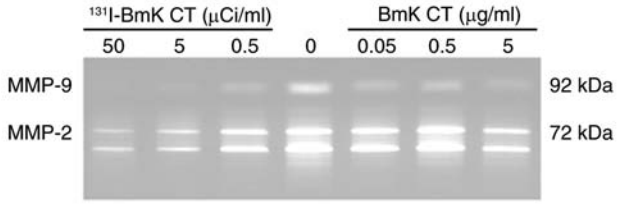

Figure 6. The activity of MMP-2 and -9 was reduced in culture supernatants secreted by U87MG cells following treatment with BmK CT or ^{131}I-BmK CT. MMP, matrix metalloproteinase; BmK CT, *Buthus martensii* Karsch chlorotoxin; ^{131}I-BmK CT, ^{131}I-labeled BmK CT.

to investigate the effect of BmK CT and ^{131}I-BmK CT on the secretion of MMP-2, MMP-9 and TIMP-2 in U87MG cells. The results demonstrated that BmK CT and ^{131}I-BmK CT inhibited the secretion of MMP-2 and -9, and stimulated the secretion of TIMP-2 in glioma cells (Fig. 5B). These results were in accordance with those of the western blotting.

^{131}I-BmK CT reduces the enzymatic activities of MMP-2 and -9 that are secreted by U87MG cells. The enzymatic activities of MMP-2 and -9 in the treated groups were analyzed and compared with the blank control using gelatin zymography. The activities of MMP-2 and -9 were reduced in the treated groups in a dose-dependent manner (Fig. 6), which may partially explain the inferior ability of cells to migrate and invade following treatment with BmK CT or ^{131}I-BmK CT.

Discussion

As malignant glioma is difficult to treat and recurs easily, novel therapies are urgently required. BmK CT has been identified as a small peptide that can specifically bind to glioma cells and inhibit their metastasis (21,27). Certain previous studies also demonstrated that BmK CT can inhibit proliferation glioma cells (21,24), but similar results were not obtained in the present study. The proliferation of U87MG cells treated with BmK CT (0-1,000 μg/ml) was assessed. Although the results do not demonstrate outcomes such as its anti-proliferative effect, the data demonstrated that BmK CT did not affect cell survival following 24, 48 and 72 h of treatment. These results suggest that BmK CT may be non-toxic at concentrations of ≤1,000 μg/ml. The results of the plate colony formation assay and flow cytometric analysis also supported this. The invasion and migration of U87MG cells was subsequently investigated. The Transwell invasion assay indicated that BmK CT exposure (0.05-5 μg/ml) for 24 h inhibited the invasiveness of U87MG cells in a dose-dependent manner. The wound-healing assay demonstrated that BmK CT exposure significantly inhibited U87MG cell migration. Notably, the data demonstrated that the anti-invasive effect of BmK CT on U87MG cells was not due to its cytotoxicity and that ^{131}I-BmK CT was more effective than BmK CT at inhibiting the invasion and migration of U87MG cells.

A previous study demonstrated that BmK CT displayed anti-metastatic ability and inhibited glioma cell invasion via MMP-2 (28). Invasion and metastasis are the later stages of tumor progression and are the major cause of treatment failure in patients with cancer due to the spreading of tumor cells from the localized stage to distant sites in order to form a secondary tumor (29). ECM degradation is a fundamental step in the process of tumor metastasis (30). MMPs that can degrade and remodel the ECM serve a major role in tumor growth, angiogenesis and metastasis. Without MMPs, tumor cells would be unable to cross through the ECM barriers that restrict their migration (31). MMP-2 and -9 are the key enzymes in the MMP family due to their critical role in ECM degradation (32). The enzymatic activity of MMPs is fundamental to their physiological role in tumor progression. BmK CT has been demonstrated to downregulate MMP-2 expression (28). In the present study, the western blotting results, laser scanning confocal images and ELISA results demonstrated that the levels of MMP-2 and -9 in or secreted by U87MG cells were reduced. The enzyme activities of MMP-2 and -9 were measured by gelatin zymography and the results indicated that the enzyme ability of MMP-2 and -9 to degrade gelatin was reduced.

MMPs can be regulated by TIMPs. TIMPs are the natural endogenous inhibitors of MMP proteins and the family contains four members (TIMP-1, -2, -3 and -4) (33). Among the TIMP family, TIMP-2 serves an essential role in regulating the activities of MMP-2 and -9. Furthermore, increasing the expression of TIMP-2 has been demonstrated to suppress cell invasion (34,35). Therefore, an aim of the present study was to investigate whether BmK CT could reduce the expression of MMP-2 and -9 through TIMP-2. The western blotting results demonstrated that TIMP-2 was increased in the U87MG cells compared with the control group, which was further supported by the laser scanning confocal images and the ELISA results, suggesting that TIMP-2 has a significant influence on the expression of MMP-2 and -9 and the invasiveness of U87MG cells. These results indicate that the BmK CT may downregulate MMP-2 and -9 by upregulating TIMP-2.

^{131}I has been widely used for the therapy of patients with cancer (36-38). Its therapeutic effect is due to its β radiation, whereas the γ rays can be used for SPECT imaging. The β emission results in the production of free radicals and toxic substances that can damage crucial macromolecules, including DNA, cell membranes and enzymes, and can cause cell death (39). These functions allow the combination of targeted tumor-specific agents to this radionuclide. Due to the high affinity to thyroid, ^{131}I has been routinely used in radionuclide therapy and imaging of thyroid diseases, especially thyroid cancer (37,40), and ^{131}I whole-body SPECT imaging has been developed as a diagnostic method in detecting recurrences or metastases from thyroid carcinoma (41). Clinical trails have demonstrated the safety of ^{131}I-labeled CTX used in the treatment of glioma patients (19,20). As a CTX-like peptide, ^{131}I-BmK CT will likely not affect normal tissues. However, some relative experiments should be performed to elucidate the safety and radiation dose *in vivo* which will be reported in our further work. In the present study, it was demonstrated that not only can ^{131}I-BmK CT inhibit metastasis, but it can also induce cell apoptosis. Although there was no obvious advantage in the effectiveness of ^{131}I-BmK CT at downregulating MMP-2 and -9 by upregulating TIMP-2 compared with BmK CT, it was more effective in reducing the enzyme abilities of MMP-2 and -9. The CCK-8 and plate colony formation assays demonstrated that ^{131}I-BmK CT had a marked effect on U87MG cell proliferation. The effect of ^{131}I-BmK CT on the

cell cycle was analyzed and the cells were demonstrated to be arrested in the S phase. The main reason that ^{131}I-BmK CT demonstrated a stronger effect than BmK CT was due to the presence of ^{131}I emitting the β minus that may induce cell apoptosis and inhibit the invasion and migration of U87 cells. This finding is consistent with a previous study, which demonstrated that ^{131}I-BmK CT significantly induced cell apoptosis (22). Induction of cell apoptosis by ^{131}I-BmK CT is a good explanation for its superior inhibitory effect on glioma cell invasion. In the present study, the effectiveness of BmK CT and ^{131}I-BmK CT at regulating MMP-2, MMP-9 and TIMP-2 were similar due to the presence of BmK CT. Following ^{131}I radiolabeling, ^{131}I-BmK CT induced apoptosis and fewer cells passing through the membrane in the Transwell invasion assay were observed, which was in accordance with the results of the wound healing assay.

Tumor-specific radionuclide therapy ensures the preferential accumulation of radiopharmaceuticals in tumor cells and not in normal tissue. As a monotherapy, BmK CT could inhibit metastasis and ^{131}I-BmK CT could be used in imaging and therapy of malignant glioma. Following BmK CT binding to glioma cells (15), the β radiation from ^{131}I induces cell death. This therapeutic method could increase the radiation reaching tumor tissues, decrease the radioactive damage to surrounding tissues and reduce the chance of relapse. However, the effect of ^{131}I-BmK CT in glioma therapy *in vivo* requires investigation in future studies.

In conclusion, the present study demonstrated that BmK CT inhibits U87MG cell metastasis, invasion and migration by downregulating MMP-2 and -9 expression and upregulating TIMP-2 expression. Additionally, BmK CT and ^{131}I-BmK CT are able to suppress the activities of MMP-2 and -9. Therefore, ^{131}I-BmK CT may be a promising therapeutic treatment for malignant glioma. ^{131}I is suitable for imaging and dose determination purposes and is simple to conjugate. In order to further determine the mechanism of the effect of BmK CT on glioma cell invasion, *in vivo* studies are required.

Acknowledgements

Not applicable.

Funding

The present study was supported by the National Natural Science Foundation of China (grant nos. 81671712 and 81401440), Shanghai Sailing Program (grant no. 16YF1409300) and West China First-Class Disciplines Basic Medical Sciences at Ningxia Medical University (grant no. NXYLXK2017B07). The present study was also supported by the platform of Shandong Co-Innovation Center of Classic TCM Formula, Scientific Innovation Team of Shandong University of Traditional Chinese Medicine, Shandong Province University Scientific Research Project (grant no. J18KZ014).

Availability of data and materials

The datasets generated and/or analyzed during the current study are available from the corresponding author on reasonable request.

Authors' contributions

WLQ and JHZ conceived and designed the experiments. SW, KM, LZZ and MLZ performed the experiments. CCL and LLG analyzed the data. YX provided the analysis tools. SW and LZZ wrote the manuscript. MLZ and JHZ edited and proofread this manuscript. All authors read and approved the final manuscript.

Ethics approval and consent to participate

Not applicable.

Patient consent for publication

Not applicable.

Competing interests

The authors declare that they have no competing interests.

References

1. Goodenberger ML and Jenkins RB: Genetics of adult glioma. Cancer Genet 205: 613-621, 2012.
2. Cuddapah VA, Robel S, Watkins S and Sontheimer H: A neurocentric perspective on glioma invasion. Nat Rev Neurosci 15: 455-465, 2014.
3. Franceschi E, Tosoni A, Girardi F and Brandes AA: Bevacizumab in brain tumors: Ready for primetime? Future Oncol 5: 1183-1184, 2009.
4. Yu Z, Zhao G, Zhang Z, Li Y, Chen Y, Wang N, Zhao Z and Xie G: Efficacy and safety of bevacizumab for the treatment of glioblastoma. Exp Ther Med 11: 371-380, 2016.
5. Hou LC, Veeravagu A, Hsu AR and Tse VC: Recurrent glioblastoma multiforme: A review of natural history and management options. Neurosurg Focus 20: E5, 2006.
6. Coussens LM, Fingleton B and Matrisian LM: Matrix metalloproteinase inhibitors and cancer: Trials and tribulations. Science 295: 2387-2392, 2002.
7. Fidler IJ, Kim SJ and Langley RR: The role of the organ microenvironment in the biology and therapy of cancer metastasis. J Cell Biochem 101: 927-936, 2007.
8. Stetler-Stevenson WG: Dynamics of matrix turnover during pathologic remodeling of the extracellular matrix. Am J Pathol 148: 1345-1350, 1996.
9. Kessenbrock K, Plaks V and Werb Z: Matrix metalloproteinases: Regulators of the tumor microenvironment. Cell 141: 52-67, 2010.
10. Figueira RC, Gomes LR, Neto JS, Silva FC, Silva ID and Sogayar MC: Correlation between MMPs and their inhibitors in breast cancer tumor tissue specimens and in cell lines with different metastatic potential. BMC Cancer 9: 20, 2009.
11. Shimoda M, Jackson HW and Khokha R: Tumor suppression by stromal TIMPs. Mol Cell Oncol 3: e975082, 2016.
12. Groblewska M, Siewko M, Mroczko B and Szmitkowski M: The role of matrix metalloproteinases (MMPs) and their inhibitors (TIMPs) in the development of esophageal cancer. Folia Histochem Cytobiol 50: 12-19, 2012.
13. DeBin JA and Strichartz GR: Chloride channel inhibition by the venom of the scorpion Leiurus quinquestriatus. Toxicon 29: 1403-1408, 1991.
14. Lyons SA, O'Neal J and Sontheimer H: Chlorotoxin, a scorpion-derived peptide, specifically binds to gliomas and tumors of neuroectodermal origin. Glia 39: 162-173, 2002.
15. Deshane J, Garner CC and Sontheimer H: Chlorotoxin inhibits glioma cell invasion via matrix metalloproteinase-2. J Biol Chem 278: 4135-4144, 2003.
16. Soroceanu L, Gillespie Y, Khazaeli MB and Sontheimer H: Use of chlorotoxin for targeting of primary brain tumors. Cancer Res 58: 4871-4879, 1998.
17. Hockaday DC, Shen S, Fiveash J, Raubitschek A, Colcher D, Liu A, Alvarez V and Mamelak AN: Imaging glioma extent with ^{131}I-TM-601. J Nucl Med 46: 580-586, 2005.

18. Shen S, Khazaeli M, Gillespie GY and Alvarez VL: Radiation dosimetry of ^{131}I-chlorotoxin for targeted radiotherapy in glioma-bearing mice. J Neurooncol 71: 113-119, 2005.
19. Mamelak AN, Rosenfeld S, Bucholz R, Raubitschek A, Nabors LB, Fiveash JB, Shen S, Khazaeli MB, Colcher D, Liu A, *et al*: Phase I single-dose study of intracavitary-administered iodine-131-TM-601 in adults with recurrent high-grade glioma. J Clin Oncol 24: 3644-3650, 2006.
20. Cheng YJ, Zhao JH, Qiao WL and Chen K: Recent advances in diagnosis and treatment of gliomas using chlorotoxin-based bioconjugates. Am J Nucl Med Mol Imaging 4: 385-405, 2014.
21. Fan S, Sun Z, Jiang D, Dai C, Ma Y, Zhao Z, Liu H, Wu Y, Cao Z and Li W: BmKCT toxin inhibits glioma proliferation and tumor metastasis. Cancer Lett 291: 158-166, 2010.
22. Zhao JH, Qiao WL, Zhang Y and Shao X: Preparation and in vitro evaluation of ^{131}I-BmK CT as a glioma-targeted agent. Cancer Biother Radiopharm 25: 353-359, 2010.
23. Qiao WL, Zhao JH, Shao X, Zhang Z, Liu X, Wang T, Jin W and Yao Y: Preparation of ^{131}I-BmK CT and bio-distribution and imaging in glioma-bearing rats. Nucl Tech 34: 213-216, 2011.
24. Fu YJ, Yin LT, Liang AH, Zhang CF, Wang W, Chai BF, Yang JY and Fan XJ: Therapeutic potential of chlorotoxin-like neurotoxin from the Chinese scorpion for human gliomas. Neurosci Lett 412: 62-67, 2007.
25. Fu YJ, An N, Chan KG, Wu YB, Zheng SH and Liang AH: A model of BmK CT in inhibiting glioma cell migration via matrix metalloproteinase-2 from experimental and molecular dynamics simulation study. Biotechnol Lett 33: 1309-1317, 2011.
26. Steeg PS: Tumor metastasis: Mechanistic insights and clinical challenges. Nat Med 12: 895-904, 2006.
27. Mignatti P and Rifkin DB: Biology and biochemistry of proteinases in tumor invasion. Physiol Rev 73: 161-195, 1993.
28. Sternlicht MD and Werb Z: How matrix metalloproteinases regulate cell behavior. Annu Rev Cell Dev Biol 17: 463-516, 2001.
29. Kim SK, Kang SW, Park HJ, Ban JY, Oh CH, Chung JH, Oh IH, Cho KB and Park MS: Meta-analysis of association of the matrix metalloproteinase 2 (-735 C/T) polymorphism with cancer risk. Int J Clin Exp Med 8: 17096-17101, 2015.
30. Schulz R: Intracellular targets of matrix metalloproteinase-2 in cardiac disease: Rationale and therapeutic approaches. Annu Rev Pharmacol Toxicol 47: 211-242, 2007.
31. Valente P, Fassina G, Melchiori A, Masiello L, Cilli M, Vacca A, Onisto M and Santi L, Stetler-Stevenson WG and Albini A: TIMP-2 over-expression reduces invasion and angiogenesis and protects B16F10 melanoma cells from apoptosis. Int J Cancer 75: 246-253, 1998.
32. Su Y, Wan D and Song W: Dryofragin inhibits the migration and invasion of human osteosarcoma U2OS cells by suppressing MMP-2/9 and elevating TIMP-1/2 through PI3K/AKT and p38 MAPK signaling pathways. Anticancer Drugs 27: 660-668, 2016.
33. Schlumberger M, Catargi B, Borget I, Deandreis D, Zerdoud S, Bridji B, Bardet S, Leenhardt L, Bastie D, Schvartz C, *et al*: Strategies of radioiodine ablation in patients with low-risk thyroid cancer. N Engl J Med 366: 1663-1673, 2012.
34. Gruenwald F and Ezziddin S: ^{131}I-Metaiodobenzylguanidine therapy of neuroblastoma and other neuroendocrine tumors. Semin Nucl Med 40: 153-163, 2010.
35. Klutz K, Schaffert D, Willhauck MJ, Gruenwald GK, Haase R, Wunderlich N, Zach C, Gildehaus FJ, Senekowitsch-Schmidtke R, Goeke B, *et al*: Epidermal growth factor receptor-targeted ^{131}I-therapy of liver cancer following systemic delivery of the sodium iodide symporter gene. Mol Ther 19: 676-685, 2011.
36. Kayano D, Kinuya S: Current consensus on I-131 MIBG therapy. Nucl Med Mol Imaging 52: 254-265, 2018.
37. Sgouros G, Kolbert KS, Sheikh A, Pentlow KS, Mun EF, Barth A, Robbins RJ and Larson SM: Patient-specific dosimetry for ^{131}I thyroid cancer therapy using ^{124}I PET and 3-dimensional-internal dosimetry (3D-ID) software. J Nucl Med 45: 1366-1372, 2004.
38. Zhang X, Liu DS, Luan ZS, Zhang F, Liu XH, Zhou W, Zhong SF and Lai H: Efficacy of radioiodine therapy for treating 20 patients with pulmonary metastases from differentiated thyroid cancer and a meta-analysis of the current literature. Clin Transl Oncol 20: 928-935, 2018.
39. Hosseinimehr SJ: Flavonoids and genomic instability induced by ionizing radiation. Drug Discov Today 15: 907-18, 2010.
40. Leo M, Sabini E, Ionni I, Sframeli A, Mazzi B, Menconi F, Molinaro E, Bianchi F, Brozzi F, Santini P, *et al*: Use of low-dose radioiodine ablation for Graves' orbitopathy: Results of a pilot, perspective study in a small series of patients. J Endocrinol Invest 41: 357-361, 2018.
41. Spanu A, Solinas ME, Chessa F, Sanna D, Nuvoli S and Madeddu G: ^{131}I SPECT/CT in the follow-up of differentiated thyroid carcinoma: Incremental value versus planar imaging. J Nucl Med 50: 184-90, 2009.